

Short Communication

Porphyrin Loading of Lipofuscin Granules in Inflamed Striated Muscle

Charles R. Kiefer,* James B. McKenney,[†]
Jane F. Trainor,[†] Richard W. Lambrecht,[‡]
Herbert L. Bonkovsky,^{‡§} Lawrence M. Lifshitz,[¶]
C. Robert Valeri,^{||} and L. Michael Snyder*

From the Departments of Hospital Laboratories/Clinical Pathology,* Pathology,[†] Medicine (and The Center for Study of Disorders of Iron and Porphyrin Metabolism),[‡] Biochemistry and Molecular Biology,[§] Physiology (and The Biomedical Imaging Group),[¶] University of Massachusetts Medical Center, Worcester, Massachusetts, and The Naval Blood Research Laboratory,^{||} Boston University School of Medicine, Boston, Massachusetts

To further the understanding of oxidative effects on inflammation injury to muscle fiber structure, fluorescent imaging analysis of human striated muscle tissues from a variety of inflammatory or postinflammatory etiologies was undertaken in a search for accumulated coproporphyrin, a red autofluorescent byproduct of heme biosynthesis that would theoretically be formed under oxidative insult. Using a differential excitation method of *in situ* analysis, porphyrin autofluorescence was detected in intact fibers within the context of the yellow autofluorescent subsarcolemmal lipofuscin granules. Relative measurements of porphyrin concentration in the granules from different patients indicated that the acute/subacute inflammatory specimens grouped significantly higher than the more chronic inflammatory and nonpathological specimens. Myoglobin was also found to be associated with the granules. Myoglobin heme iron could potentially serve as a Fenton reagent for the intracellular generation of hydroxyl radicals, which are responsible for the oxidation of the porphyrinogens. High-performance liquid chromatography analysis of extracted dense particles revealed coproporphyrin as the sole porphyrin present. The observation of coproporphyrin within lipofuscin granules, previously unreported, suggests that lipofuscin accumulation in striated muscle may begin under conditions of acute oxidative stress, as marked by the oxidation of extramitochondrial porphyrinogens that are immediately incorporated into the granules. (Am J Pathol 1998, 153:703–708)

The myoglobin-loaded red fibers of striated muscle would theoretically seem to be especially susceptible to free radical damage in an inflammatory response. Reactive oxygen intermediates are released by neutrophils and/or monocytes/macrophages as one class of many nonspecific defense mediators to contain infection. Inflammatory responses also occur on re-establishment of blood flow into tissue temporarily deprived of circulation (reperfusion injury after ischemia). Accumulating evidence suggests that reperfusion injury to both the microvascular and parenchymal components of muscle is mediated by reactive oxygen intermediates released by tissue infiltrating neutrophils.^{1–3} Inside the fiber, myoglobin heme iron could conceivably serve as a catalytic source of hydroxyl radical generation in a Fenton reaction driven by the released peroxides crossing the muscle fiber membrane (sarcolemma).⁴ A natural visible indication of oxidative damage within the muscle fiber might result from the oxidation of extramitochondrial nonfluorescent porphyrinogens to their fluorescent porphyrin counterparts, which can be mediated by hydroxyl radicals, as demonstrated *in vitro*.⁵ The attack of hydroxyl radicals on alkyl carbons is electrophilic, and the predominant reaction is hydrogen abstraction.⁶ Thus, hydroxyl radicals could oxidize the methylene bridges of the porphyrinogens to the methene bridges that characterize the porphyrins. By way of analogy, in hepatic cells, iron increases oxidative stress and enhances the oxidation of porphyrinogens to porphyrins.⁷ Iron has been shown to be a major triggering factor in the development of biochemically and clinically overt porphyria cutanea tarda,^{7,8} in which uroporphyrin crystals in hepatic cells have been localized to regions with dense ferritin granule deposition.⁹

Supported by the US Navy (Office of Naval Research Contract No. N00014-79-C-168, with funds provided by the Naval Medical Research and Development Command), and the US Public Health Service (National Institutes of Health grant DK 38825 to HLB).

Accepted for publication May 30, 1998.

Address reprint requests to Dr. Charles R. Kiefer, UMass Memorial Health Care, University Campus, Department of Hospital Labs/Clinical Pathology, 55 Lake Avenue North, Worcester, MA 01655-0220. E-mail: charles.kiefer@banyan.ummed.edu.

Coproporphyrin is the porphyrin type excreted in patients with muscle damage resulting from ischemia or infarction.¹⁰ Reasoning that coproporphyrin excretion probably follows an acute intracellular accumulation, we examined biopsied specimens of striated muscle from a variety of human inflammatory conditions, acute and chronic (inflammatory myopathies and acute and chronic occlusive vascular disease of skeletal and cardiac muscle), for evidence of coproporphyrin accumulations. We also studied heart muscle from a rat model of acute cardiac ischemia.

Materials and Methods

Human Striated Muscle Specimens

Skeletal and cardiac muscle specimens (from biopsy, amputation, and autopsy), and histopathological diagnoses where indicated, were obtained through the Division of Anatomic Pathology, University of Massachusetts Medical Center. For control specimens, normality was evaluated through hematoxylin and eosin-stained paraffin sections as well as frozen sections and were defined by findings of normal size variability and configuration relative to the patient's age; no specific abnormalities; no fiber degeneration/regeneration, atrophy or hypertrophy, inflammation, or vasculitis; and no myopathic changes, including fiber splitting, ring fibers, or fibrosis.

Rat Muscle Specimens

Experimental myocardial infarction was induced in rats by isoproterenol injection.¹¹ Briefly, a 500-g male Wistar rat was injected with 100 mg isoproterenol/kg s.c. The animal was euthanized under halothane anesthesia 24 hours later, and the heart was excised and immediately frozen in liquid nitrogen cooled isopentane. A control rat heart was obtained from an untreated animal of the same weight, sex, and strain. The care and use of the animals was in accordance with institutional guidelines.

Digital Imaging Microscopy (DIM)

The microscopic methods have been described previously.^{12,13} Briefly, specimens were cut in 10 μm -thick cross-sections, adhered to glass slides, air-dried, acetone-fixed, and mounted in 50% glycerol, 2.5% 1,4-diazabicyclo[2.2.2]octane in 5 mmol/L phosphate buffer, pH 8. For DIM analysis, the mounted specimen was optically sectioned (at $\times 150$) in 0.25- μm planes using a standard wide-field microscope, and the optical data were digitized by a cooled charge-coupled device (CCD) camera into a 310 \times 510-pixel format. Point-spread functions (PSFs) to establish a three-dimensional standard for removing out-of-focus light were acquired by using tetramethyl rhodamine-conjugated 0.1- μm fluorescent beads. Dark current images (*DC*) to compensate for instrument background were acquired for both the specimens and PSFs using the same parameters as for the corresponding specimen images. Flat field images (*FF*), acquired

with a rhodamine-conjugated immunoglobulin G (IgG) solution, were used to control for CCD sensitivity. The measured fluorescent intensity of this intermediate stage image (*I*) was calculated from $(I-DC)/FF$. Finally, image restoration (deconvolution) algorithms were used to remove out-of-focus light from the sections, improving resolution and contrast.

Calculation of Relative Porphyrin Content of Lipofuscin (LF) Granules

Sectioned muscle specimens were first examined with a filter set designed to maximally excite both porphyrin and LF (broad-range excitation filter 390 to 490 nm, 500-nm long pass dichroic extended reflection filter, and porphyrin emission filter 585 to 635-nm), and the optical data were captured by a CCD camera. The same field was then reexamined after changing the excitation filter (420 to 490 nm), which eliminated that section of the LF excitation range that also excited porphyrin. Both excitation filters allowed the same degree of light transmission (80%) within their wavelength ranges. The CCD images were then restored, aligned, and displayed. Individual granules were manually segmented from the field and integrated three dimensionally to determine the total fluorescence intensities for each filter set. The mean ratio $(PE + fLF)/fLF$ (described below) was calculated from a minimum of three granules for each specimen. All specimens were cut from frozen tissue stored for less than 3 years at -70°C . The order of capturing the image sets on the CCD camera was always the same. Both coproporphyrin and LF are relatively slow-bleaching, LF more so than coproporphyrin. For this reason, data from the broad range excitation filter, which would include the porphyrin component, were obtained first.

The expression $(PE + fLF)/fLF$ is derived from $[I/(PE + f'LF + fLF)]/[I/(fLF)]$, where *I* represents fluorescence intensity, *PE* represents the full emission of optimally excited porphyrin (excitation, 390 to 420 nm; emission, 585 to 635 nm), *f'LF* represents a marginal emission of optimally excited LF (excitation, 390 to 490 nm; emission, 585 to 635 nm), and *fLF* represents a marginal emission of suboptimally excited LF (excitation, 420 to 490 nm; emission, 585 to 635 nm). The assumption is made that LF fluorescence at 585 to 635 nm resulting from LF excitation at 390 to 420 nm (ie, *f'LF*) is very small relative to *PE*. This is not an unreasonable assumption, because probable LF fluorophores that are likely to be excited in this range, the 1,4-dihydropyridine-3,5-dicarbaldehydes, emit at 435 to 465 nm.¹⁴ Thus, the original expression reduces to $I/(PE + fLF)/I/(fLF)$, or $(PE + fLF)/fLF$.

Immunohistochemical Detection of Myoglobin within LF Granules

Anti-myoglobin monoclonal antibody M-2-167 (IgG1)¹⁵ and anti- α spectrin ($\alpha 1\Sigma 1$) monoclonal antibody bs α -4-119 (IgG1)¹⁶ were used at 0.1 $\mu\text{mol/L}$ in conjunction with a cy5-conjugated goat anti-mouse IgG1 (product code

M32011, Caltag Laboratories, South San Francisco, CA). Immunofluorescent intensities were calculated by computational summation of planar intensities, one pixel thick, constructed perpendicular to an arbitrary axis through the granule. The cy5/baseline values derived for each granule represent the immunofluorescent (cy5) total granule intensity (excitation, 620 to 660 nm; emission, 665 to 695 nm) divided by a baseline autofluorescent total granule intensity (excitation, 515 to 565 nm; emission, 577.5 to 632.5 nm).

Extraction and Analysis of Porphyrins from Autofluorescent Dense Particles

In our modification of a previously published procedure,¹⁷ 3 g muscle tissue was homogenized with 9 ml of 10 mmol/L phosphate buffer (pH 7.4), 1 mmol/L ethylenediaminetetraacetic acid, protease inhibitors, and 1% Triton X-100. After centrifuging at $1,000 \times g$ for 10 minutes, the supernatant was recovered, recentrifuged, and separated from the floating lipids by collection from the bottom (tube puncture). It was then layered over 30% sucrose and centrifuged at $40,000 \times g$ for 90 minutes. A fraction of the pelleted material was checked by DIM and found positive for porphyrin and LF autofluorescence. A proportion of the pelleted material (1g-equivalent muscle wet weight) was then extracted with the acetone:HCl/ether:HCl system referenced above to yield hemin-free porphyrins that were dried, solubilized in 0.1 N HCl, and analyzed by reversed-phase high-performance liquid chromatography.

Results

Localization of Porphyrin Accumulations to Subsarcolemmal Granules

Examinations for porphyrin accumulations were conducted by DIM. In the human inflammatory specimens, porphyrin-range autofluorescence was found to associate with subsarcolemmal granule-like structures, often occurring in clusters (Figure 1A). Such structures were found much less frequently in nonpathological specimens from individuals at least 6 years old and were topographically simpler and of less fluorescent intensity (Figure 1, D versus B). The structures were not present in a nonpathological specimen from a 1-year-old child (not shown). The structures were found to be prevalent in a human specimen of acute ischemic cardiac muscle (Figure 2A), but were no more prevalent than in specimens from chronic vasoocclusive cardiac muscle (not shown). In the muscle of freshly amputated lower legs with chronic vascular occlusive disease and gangrene, the structures were prevalent, although the muscle fiber integrity was typically in poor shape (not shown). Similar structures were observed in rat acute ischemic cardiac muscle (Figure 2B) but not in controls (not shown). The apparent correlation of the number and size of these structures with age, and their subsarcolemmal location,

suggested their association with muscle LF granules, the subsarcolemmal yellow autofluorescent age pigment.

Porphyrin Accumulations as a Function of Inflammatory Status

To determine whether porphyrin accumulation was increased in inflamed muscle tissue, we sought to measure, *in situ*, the porphyrin content per unit volume of LF. LF fluorescence is best measured by using a broad-range excitation filter (390 to 490 nm) with a 515-nm barrier filter.¹⁴ The emission peak for LF in muscle is within the 510 to 530-nm range,¹⁸ although its fluorescence extends into the porphyrin range.¹⁴ Porphyrin fluorescence peaks at 600 to 630 nm and is characteristically excited at wavelengths near 400 nm.¹⁰ Thus, excitation of porphyrin would also excite LF to some extent, the fluorescence from which would overlap somewhat that of porphyrin. A relative measure of porphyrin within an LF context could be calculated from porphyrin-range fluorescence intensities at two excitation ranges. The range 390 to 490 nm would maximally excite both porphyrin and LF, and the range 420 to 490 should excite a major fraction of LF but very little of porphyrin. For any given granule, the ratio of these two fluorescence intensities could be expressed as $(PE + fLF)/fLF$ (a ratio of porphyrin to lipofuscin spillover), where *PE* represents fluorescence due to porphyrin, and *fLF* represents the suboptimally excited, marginal LF fluorescence within the porphyrin emission range.

Using this differential excitation method, Table 1 shows significantly elevated ratios for specimens of acute inflammatory skeletal muscle and acute ischemic cardiac muscle versus those found in more chronic inflammatory/ischemic or nonpathological striated muscle, indicating porphyrin loading of LF granules during acute inflammatory episodes. To determine whether the distribution of porphyrin within the LF granule was either homogeneous or shell-like, cross-sectional analysis of individual granules from the adult dermatomyositis specimen was performed. The Gaussian-like curves of both signals (Figure 3) indicated fairly homogeneous distributions (a predominantly bimodal curve would have indicated a shell-like distribution). It is noteworthy that loading of porphyrin into LF granules can occur rapidly under conditions of experimental acute cardiac ischemia (Figure 2B).

Identification of Porphyrin Type

LF granules exhibit a density of 1.140 to 1.178 g/cm³.¹⁹ In an attempt to isolate porphyrins associated with these granules, chronic vaso-occlusive muscle samples from both amputated leg and autopsied heart (Table 1, specimen 7) were solubilized and an autofluorescent-dense (>1.132 g/cm³) particulate fraction (checked by DIM) was extracted using a solvent system designed to isolate hemin-free porphyrins.¹⁷ The isolates were then examined for spectral excitation and emission characteristics and checked for high-performance liquid chromatography retention time in comparison with porphyrin stan-

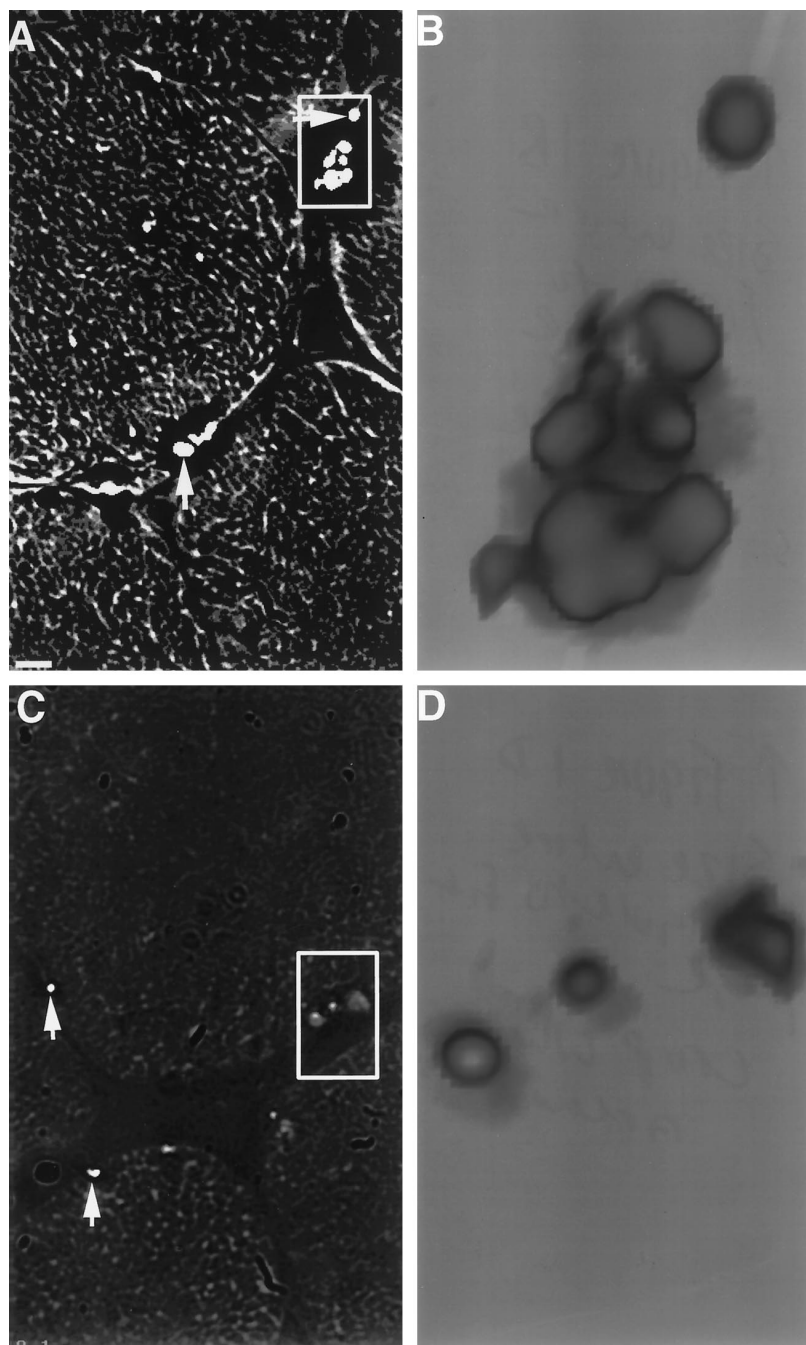


Figure 1. Red fluorescent granules in human skeletal muscle. Frozen muscle biopsy specimens were sectioned and analyzed by DIM. To induce and detect maximal fluorescence of accumulated porphyrin, excitation (400 to 410 nm) and emission (585 to 635 nm) filter ranges were chosen on the basis of excitation and emission scans of soluble purified coproporphyrin III (Porphyrin Products, Logan, UT). In A and C, single restored optical planes (150 \times) are presented to better demonstrate the location of the autofluorescent granules (arrowheads) within the structural context of the muscle fibers. In B and D, segments of A and C, respectively, are presented in their three-dimensional restored forms. The black/white context is reversed to better visualize the topography of the granules. A: Specimen from a 43-year-old male with dermatomyositis (bar = 5 μ m). B: Three-dimensional restoration of a segment of A. C: Specimen from a normal 24-year-old male. D: Three-dimensional restoration of a segment of C.

dards. By these criteria, the isolates were found to be the same from both skeletal and cardiac tissue. The extracted porphyrin exactly resembled coproporphyrin III in both spectral characteristics ($\lambda_{\text{excite}} = 406.0$ nm; $\lambda_{\text{emit}} = 604.8$ and 607.9 nm) and high-performance liquid chromatography retention time (single peak, 10.80 minutes, versus 10.78 minutes for coproporphyrin III standard).

Presence of Myoglobin within the Porphyrin/LF Granules

The autofluorescence of LF granules poses obvious special problems for the immunofluorescent detection of specific antigens of interest, requiring a quantitative ap-

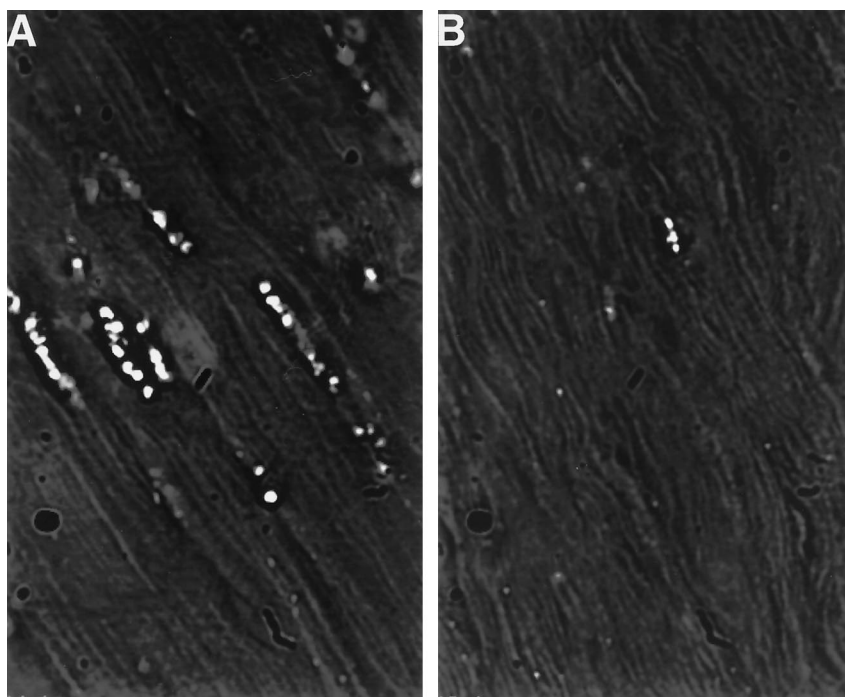


Figure 2. Red fluorescent granules in cardiac muscle. Frozen specimens of cardiac tissue were examined (150 \times) for the presence of accumulated porphyrin as described in Figure 1. **A:** Autopsy specimen from a 29-year-old female (left ventricle infarction associated with disseminated intravascular coagulation). **B:** Rat cardiac muscle taken 24 hours after induction of acute cardiac ischemia by isoproterenol.

proach that controls for LF fluorescent background within the fluorescent emission range of the immunospecific signal. To determine whether myoglobin (and presumably heme iron) associated *in situ* with the porphyrin/LF granules, we set up a quantitative immunofluorescent DIM assay. Mouse monoclonal antibodies of the same isotype (IgG1) were used to detect the presence of myoglobin and the absence of α spectrin ($\alpha 1\Sigma 1$ isoform), the latter expressed only in red cells and thus a negative control. Because the overall autofluorescence of the granules was less intense in the far red region, despite the contribution of coproporphyrin, we chose cy5 as the fluorescent reporter conjugated to the second antibody, an affinity-purified antimouse IgG1. To normalize the immunofluorescent data collected from eight individual

granules per assay, we calculated the ratio of immunofluorescent intensity observed with the cy5 signal divided by that observed for a baseline intensity closer to the autofluorescent peak of LF. The latter was accomplished by using a tetramethyl rhodamine filter set, for which the excitation range does not overlap that of cy5. By such an analysis (Table 2), we determined that myoglobin was associated with the granules ($P < 0.01$, *t*-test).

Discussion

Although it has generally been understood that LF formation in striated muscle is a gradual, age-related process,¹⁴ the data presented suggest that porphyrin-

Table 1. Porphyrin Loading of LF Granules as a Function of Inflammatory Status

Group (specimen no.)	(PE + fLF)/fLF (SD)
Group 1 (acute inflammation)	
(1) Dermatomyositis skeletal muscle, 43-year-old male	2.34 (0.04)
(1) Dermatomyositis skeletal muscle, 43-year-old male (<i>N</i> = 6)	2.32 (0.06)
(2) Dermatomyositis skeletal muscle, 4-year-old male	1.83 (0.04)
(3) Acute ischemic cardiac muscle, 29-year-old female	1.85 (0.05)
Group 2 (chronic inflammation and nonpathological muscle)	
(4) Chronic vaso-occlusive skeletal muscle, 72-year-old female	1.71 (0.03)
(5) Chronic vaso-occlusive skeletal muscle, 87-year-old female	1.45 (0.02)
(6) Chronic vaso-occlusive skeletal muscle, 90-year-old female	1.25 (0.05)
(7) Chronic ischemic cardiac muscle, 73-year-old male	1.35 (0.03)
(8) Normal (nonpathological) skeletal muscle, 66-year-old male	1.40 (0.12)
(9) Normal (nonpathological) skeletal muscle, 24-year-old male	1.31 (0.10)
(10) Normal (nonpathological) skeletal muscle, 6-year-old male	1.34 (0.05)

Certain of these specimens are shown in the figures (specimen 1, Figure 1, A and B; specimen 3, Figure 2A; specimen 9, Figure 1, C and D). Measurements are the means (and standard deviations) of the porphyrin/LF spillover fluorescence ratios for three granules per specimen, except as noted. The mean (PE + fLF)/fLF values of the two groups are significantly different ($P < 0.01$, *t*-test).

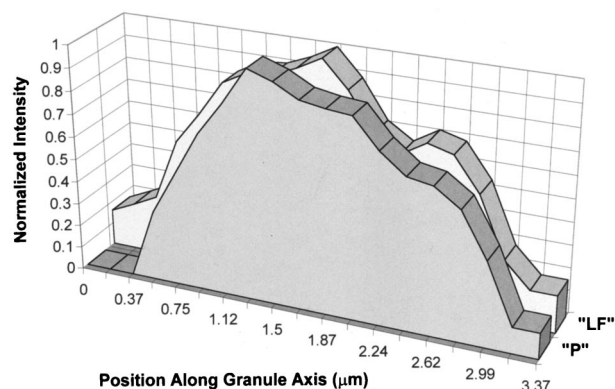


Figure 3. Cross-sectional analysis of porphyrin/LF granules for distribution of fluorescent signals. DIM data from dermatomyositis skeletal muscle specimen (Table 1, specimen 1) was collected for porphyrin plus partial LF fluorescence ("P": excitation 400 to 410 nm; 415-nm long-pass dichroic; emission, 585 to 635 nm) and for suboptimal LF fluorescence exclusive of porphyrin ("LF": excitation, 420 to 490 nm; 500-nm long-pass dichroic extended reflection; emission, 520 nm long-pass barrier filter). Presented here is a single granule from the field that was computationally analyzed for fluorescence intensity of each signal in sequential planes 1 pixel thick (0.187 µm) constructed perpendicular to an arbitrary axis through the granule. Results are presented as planar fluorescence intensity (normalized to 1.0 for each signal) versus position (µm) along the granule axis.

Table 2. Association of Myoglobin with Porphyrin/LF Granules

Assay	cy5/baseline (SD)
Myoglobin	0.1402 (0.0508)
α-Spectrin (control)	0.0808 (0.0065)

This specimen is shown in Figure 1, A and B. Measurements are the means (and standard deviations) of normalized immunofluorescent intensities for eight granules per assay. The mean values of the two groups are significantly different ($P < 0.01$, *t*-test).

loaded LF granules may also form within an acute oxidative context. Although conclusions cannot be directly extrapolated to humans from the experimental rat model (Figure 2B), the relative porphyrin content of LF granules in human skeletal muscle (Table 1), as well as their prevalence (Figure 1, A versus C), directly correlates with recent inflammatory history. The association of myoglobin with the granules (Table 2) supports the hypothesis that heme iron-catalyzed generation of hydroxyl radicals may play a role in the oxidation of cytoplasmic porphyrinogens and their loading into the granules.

Acknowledgment

We thank Dr. Eric Dickson, Department of Emergency Medicine, University of Massachusetts Medical Center,

for technical expertise with the rat myocardial infarction model.

References

- Korthuis RJ, Granger DN, Townsley MI, Taylor AE: The role of oxygen-derived free radicals in ischemia-induced increases in canine skeletal muscle vascular permeability. *Circ Res* 1985, 57:599-609
- Odeh M: The role of reperfusion-induced injury in the pathogenesis of the crush syndrome. *N Engl J Med* 1991, 324:1417-1422
- Formigli L, Lombardo LD, Adembri C, Brunelleschi S, Ferrari E, Novelli GP: Neutrophils as mediators of human skeletal muscle ischemia-reperfusion syndrome. *Hum Pathol* 1992, 23:627-634
- Sadrzadeh SMH, Graf E, Panter SS, Hallaway PE, Eaton JW: Hemoglobin: a biologic Fenton reagent. *J Biol Chem* 1984, 259:14354-14356
- Smith AG, De Matteis F: Oxidative injury mediated by the hepatic cytochrome P-450 system in conjunction with cellular iron: effects on the pathway of haem biosynthesis. *Xenobiotica* 1990, 20:865-877
- Sangster DF: Free radical and electrophilic hydroxylation. *The Chemistry of the Hydroxyl Group*. Edited by S Patai. London, Interscience, 1971, pp 133-191
- Bonkovsky HL: Porphyrin and heme metabolism and the porphyrias. *Hepatology: A Textbook of Liver Disease*, ed 2. Edited by D Zakim, TD Boyer. Philadelphia, Saunders, 1990, pp 378-424
- Bonkovsky HL, Lambrecht RW: Hemochromatosis, iron overload, and porphyria cutanea tarda. *Hemochromatosis*. Edited by JC Barton, CQ Edwards. Cambridge, UK, Cambridge University Press (in press)
- Siersema PD, Rademakers LHPM, Cleton MI, ten Kate FJW, de Bruijn WC, Marx JJM, Wilson JHP: The difference in liver pathology between sporadic and familial forms of porphyria cutanea tarda: the role of iron. *J Hepatol* 1995, 23:259-267
- Eales L: Clinical chemistry of the porphyrins. *The Porphyrins*, vol 6, Biochemistry, Part A. Edited by D Dolphin. New York, Academic Press, 1979, pp 663-804
- Rona G, Chappel CI, Balazs T, Gaudry R: An infarct-like myocardial lesion and other toxic manifestations produced by isoproterenol in the rat. *AMA Arch Pathol* 1959, 67:443-455
- Lifshitz LM, Collins JA, Moore ED, Gauch J: Computer vision and graphics in fluorescence microscopy. *Proceedings of the IEEE Workshop on Biomedical Image Analysis*. Los Alamitos CA, Computer Society Press, 1994, pp 166-175
- Carrington WA, Fogarty KE, Lifshitz LM, Fay FS: Three-dimensional imaging on confocal and wide field microscope. *The Handbook of Biological Confocal Microscopy*. Edited by J Pawley. New York, Plenum Press, 1989, pp 151-161
- Yin D: Biochemical basis of lipofuscin, ceroid, and age pigment-like fluorophores. *Free Radical Biol Med* 1996, 21:871-888
- Moscoco H, Kiefer CR, Shyamala M, von Dohlen T, Garver FA: Monoclonal antibody-based immunoassays for serum myoglobin quantification in acute myocardial infarction. *J Clin Lab Anal* 1990, 4:437-442
- Kiefer CR, McKenney JB, Trainor JF, Lifshitz L, Krasnicki S, Schneider T, Schrier SL, Morrow JS, Valeri CR, Snyder LM: Hemoglobin-spectrin complexes: distribution within the erythrocyte skeleton. *Blood* 1995, 86 (Suppl 1):630a
- Healey JF, Bonkovsky HL, Sinclair PR, Sinclair JF: Conversion of 5-aminolaevulinate into haem by liver homogenates: comparison of rat and chick embryo. *Biochem J* 1981, 198:595-604
- Karpati G, Carpenter S, Wolfe LS: Clinical and experimental studies on lipofuscin in skeletal muscle fibers. *Lipofuscin-1987: State of the Art*. Edited by I Zs.-Nagy. Amsterdam, Elsevier, 1988, pp 227-244
- Bjorkerud S: Isolated lipofuscin granules: a survey of a new field. *Adv Gerontol Res* 1964, 1:257-287